Evidence for the Iron(III) Oxidation State in Bis(imino)pyridine Catalysts. A Density Functional Theory Study

Roman Raucoules,[†,‡] Theodorus de Bruin,*[,†] Pascal Raybaud,[§] and Carlo Adamo[‡]

IFP, Direction Chimie et Physico-chimie Appliquées, 1-4 Avenue de Bois Préau, 92852 Rueil-Malmaison Cedex, France, Laboratoire d'Electrochimie et de Chimie Analytique, CNRS UMR 7575, Ecole Nationale Supérieure de Chimie de Paris, 11 rue P. et M. Curie, F-75231 Paris Cedex 05, France, and IFP, Direction Catalyse et Séparation, Rond-point de l'échangeur de Solaize, BP 3, 69360 Solaize, France

Received November 7, 2007

We report a theoretical analysis based on density functional theory devoted to the study of the activated iron bis(imino)pyridine catalysts $\{[2,6\text{-}(2\text{-}C_6H_4(CH_3))_2\text{-}C_5H_3N]Fe^nR_x]^{n-x}\}$ ($n = 2, 3$; $x = 1, 2$; R = Me, Cl). The aim of this work is to obtain detailed information on the nature (oxidation state and spin multiplicity) of the iron active species, by studying the coordination and insertion of the first ethylene molecule with the 10 most reasonable activated species that can be formed out of $\{[2,6\text{-}(2\text{-}C_6H_4(CH_3))_2\text{-}C_5H_3N]FeCl_2\}$ after reaction with MAO. The relatively small exothermicity of the coordination reaction of ethylene, calculated for disubstituted species, allowed us to exclude them from further examination. The coordination and insertion reaction pathway for the two most reactive activated catalysts, i.e., monomethylated Fe(III) and Fe(II) species, were then evaluated on the B3LYP/Lacvp** potential energy surface (PES), taking into account all possible spin states and several coordination modes of the ethylene molecule. These reactions take place at the quintet PES for the Fe(II) and quartet PES for the Fe(III) species. For the latter, more favorable reaction and activation enthalpies for the insertion reaction were calculated: Fe(II), ΔH(298 K) = –14.1 kcal/mol and $\Delta H^{\ddagger}$(298 K) = +21.6 kcal/mol; Fe(III), ΔH(298 K) = −22.8 kcal/mol and $\Delta H^{\ddagger}$(298 K) = +10.0 kcal/mol. Assuming similar insertion barriers for the second insertion reaction, the β-hydrogen transfer termination reaction ($\Delta H^{\ddagger}$ = +11.9 kcal/mol) is favored over further chain growth for $[Fe^{II}Me]^+$, whereas for $[Fe^{III}Me]^{2+}$ catalyst chain growth and termination reaction are clearly in competition ($\Delta H^{\ddagger}$ = +10.0 and +12.1 kcal/mol, respectively). On the basis of these results, we conclude that the most activated species has oxidation state III and is likely expected to produce oligomers in agreement with results from experimental studies.

1. Introduction

Understanding and developing efficient catalysts for olefin oligo- and polymerization have been very important topics in chemistry during the last 50 years. In 1955 and 1956, Ziegler and Natta launched the first generation of group 4 metal based (Ti, Zr, V) catalysts active in heterogeneous olefin polymerization,[1] and Natta and Breslow showed independently in 1957 that $TiCl_2(Cp)_2$ could be activated by Et_3Al or Et_2AlCl to yield a homogeneous olefin polymerization catalyst.[2] In the late 1970s Sinn and Kaminsky reported that methylaluminoxane (MAO) is extremely efficient at activating group 4 metallocenes[3] and improved activities for α-olefin polymerizations have been reported.[4] In 1998, Brookhart and Gibson independently discovered that MAO-activated iron bis(imino)pyridine (see Scheme 1: R1, R2, R3, R4 = H, alkyls; X1 = X2 = Cl)[5] yielded activities (in particular for the conversion of ethylene into high-density polyethylene) that were as high as those of group 4 metallocenes, also activated by MAO.

Scheme 1. Labeling of the Activated Iron Bis(imino)pyridine Catalysts

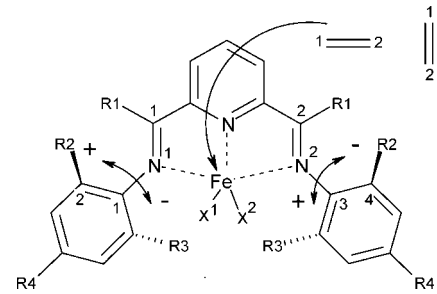

Since 2002, different research groups have shown that the oligomerization of olefins could be obtained to the detriment

* To whom correspondence should be addressed. E-mail: theodorus.debruin@ifp.fr.

† IFP, Direction Chimie et Physico-chimie Appliquées.

‡ Ecole Nationale Supérieure de Chimie de Paris.

§ IFP, Direction Catalyse et Séparation.

(1) (a) Ziegler, K.; Holzkamp, E.; Martin, H.; Breil, H. *Angew. Chem.* **1955**, *67*, 541. (b) Natta, G. *Angew. Chem.* **1956**, *68*, 393.

(2) (a) Natta, G.; Pino, P.; Mazzanti, G.; Giannini, U. *J. Am. Chem. Soc.* **1957**, *79*, 2975. (b) Breslow, D. S.; Newburg, N. R. *J. Am. Chem. Soc.* **1957**, *79*, 5072.

(3) Sinn, H.; Kaminsky, W. *Adv. Organomet. Chem.* **1980**, *18*, 99.

(4) (a) Kaminsky, W.; Miri, M.; Sinn, H.; Woldt, R. *Makromol. Chem. Rapid Commun.* **1983**, *4*, 417. (b) Brintzinger, H. H.; Fischer, D.; Mülhaupt, R.; Rieger, B.; Waymouth, R. *Angew. Chem., Int. Ed. Engl.* **1995**, *34*, 1143.

(5) (a) Small, B. L.; Brookhart, M.; Bennett, A. M. A. *J. Am. Chem. Soc.* **1998**, *120*, 4049. (b) Small, B. L.; Brookhart, M. *J. Am. Chem. Soc.* **1998**, *120*, 7143. (c) Britovsek, G. J. P.; Bruce, M.; Gibson, V. C.; Kimberley, B. S.; Maddox, P. J.; McTavish, S. J.; Solan, G. A.; White, A. J. P.; Williams, D. J. *Chem. Commun.* **1998**, 849. (d) Britovsek, G. J. P.; Bruce, M.; Gibson, V. C.; Kimberley, B. S.; Maddox, P. J.; Mastroianni, S.; McTavish, S. J.; Redshaw, C.; Solan, G. A.; Strömberg, S.; White, A. J. P.; Williams, D. J. *J. Am. Chem. Soc.* **1999**, *121*, 8728. (e) Britovsek, G. J. P.; Mastroianni, S.; Solan, G. A.; Baugh, S. P. D.; Redshaw, C.; Gibson, V. C.; White, A. J. P.; Williams, D. J.; Elsegood, M. R. J. *Chem. Eur. J.* **2000**, *6*, 2221.

10.1021/om701122r CCC: $40.75
Publication on Web 06/25/2008

of polymerization by fine-tuning the nature and the size of the substituents on the aryl groups: the presence of two substituents at the two ortho positions (i.e., R2, R3 ≠ H in Scheme 1) of the two aryl groups preferentially yields long-chain polymers, whereas with the occupation of only one ortho position (i.e., R2 ≠ H and R3 = H) selective oligomers can be produced.[6]

Today, it remains a challenging task to fully rationalize these experimental outcomes. Even more fundamentally, several studies diverge upon the exact oxidation degree of the iron ion. Gibson and co-workers accounted for Fe(III), on the basis of Mössbauer and EPR spectroscopy,[7] while the NMR and EPR studies of Talsi et al. concluded that the activation of the precatalyst by MAO results in Fe(II) species.[8] This latter conclusion was further supported by a communication of Chirik and co-workers, in which it was reported that iron dichloride precursors, after treatment with alkyllithiums and borate, yield polymers that are similar to those obtained after activation with MAO.[9] On the basis of experimental and theoretical results additional support for Fe(II) species was provided by Scott et al., who put forward that Fe(II) is coordinated to a bis(imino)pyridine ligand, which in turn is thought to possess a diradical dianion character, although the overall complex has a formal zerovalent state.[10] The diradical dianion of the ligand character was then further investigated by a computational study by Neese et al., in which it was found that electron transfer originates from a reorganization within the conjugated ligand and that there is no electron transfer from the metal center toward the ligand.[11]

Apart from the oxidation state, uncertainty also exists about the precise electronic structure of the iron species. In a theoretical study Ziegler and co-workers reported that the singlet electronic state of Fe(II) is the most favorable state for the propagation and the termination reaction.[12] Conversely, Morokuma et al.,[13] Zakharov et al.,[8] and Budzelaar and co-workers[14] found, using a different density functional theory (DFT) method, that the electronic configuration of Fe(II) in the propagation reaction corresponds to a high (i.e., quintet or triplet) spin state.

Actually, these two important characteristics of the iron center, oxidation state and electronic configuration, in the iron bis(imino)pyridine complexes have still not been fully rationalized. It is thus of great importance to have a better understanding of the precise nature of the iron reaction center, before one can address and propose reaction mechanisms that intend to explain the selective formation of certain olefins or polymers.

We present here a theoretical study in which the nature of the iron species is characterized by carefully exploring the potential energy surface for the coordination and insertion reactions of an ethylene molecule for the 10 most reasonable activated species of $\{[2,6\text{-}(2\text{-}C_6H_4(CH_3))_2\text{-}C_5H_3N]FeCl_2\}$ after reaction with MAO, whose structure cannot be precisely assessed.[15] These species differ in oxidation state, electronic configuration, and ligand (X = Me, Cl). Naturally, the two main termination reactions, i.e., β-hydrogen transfer and β-hydrogen elimination (BHE), will also be taken into account. On the basis of the energetics of these reactions, the nature of the most active species is then proposed.

2. Computational Methods

All of the DFT calculations have been performed with the functional B3LYP,[16] using its unrestricted formalism in combination with the pseudopotential LanL2DZ[17] on the iron atom and the double-ζ basis set 6-31G(d,p) on the other atoms. All geometry optimizations and frequency analysis were realized with the Jaguar[18] program using the implemented pseudospectral method.[19] Frequency analyses have been performed on all intermediates of the two most reactive species to confirm the desired character of the stationary point and to evaluate thermodynamic contributions. For these species the energy is expressed in enthalpies calculated at $T = 298$ K, whereas otherwise the electronic energy (E_{scf}) is reported. Net atomic charges are calculated using natural population analysis.[20] Self-consistent field energies for bimolecular species have been corrected for the basis set superposition error using the Counterpoise correction method.[21] Atoms-in-molecules (AIM)[22] calculations have been realized with the Morphy software.[23]

(6) (a) Ma, Z.; Sun, W.-H.; Li, Z.-L.; Shao, C.-X.; Hu, Y.-L.; Li, X.-H. *Polym. Int.* **2002**, *51*, 994. (b) Kim, I.; Han, B. H.; Ha, Y.-S.; Ha, C.-S.; Park, D.-W. *Catal. Today* **2004**, *93*−*95*, 281. (c) Chen, Y.; Chen, R.; Qian, C.; Dong, X.; Sun, J. *Organometallics* **2003**, *22*, 4312. (d) Tellmann, K. P.; Gibson, V. C.; White, A. J. P.; Williams, D. J. *Organometallics* **2005**, *24*, 280. (e) Bianchini, C.; Giambastiani, G.; Guerrero Rios, I.; Meli, A.; Passaglia, E.; Gragnoli, T. *Organometallics* **2004**, *23*, 6087. (f) Schmidt, R.; Welch, M. B.; Knudsen, R. D.; Gottfried, S.; Alt, H. G. *J. Mol. Catal. A* **2004**, *222*, 9. (g) Bianchini, C.; Mantovani, G.; Meli, A.; Migliacci, F.; Zanobini, F.; Laschi, F.; Sommazzi, A. *Eur. J. Inorg. Chem.* **2003**, 1620. (h) Galland, G. B.; Quijada, R.; Rojas, R.; Bazan, G.; Komon, Z. J. A. *Macromolecules* **2002**, *35*, 339. (i) Quijada, R.; Rojas, R.; Bazan, G.; Komon, Z. J. A.; Mauler, R. S.; Galland, G. B. *Macromolecules* **2001**, *34*, 2411. (j) Wang, H.; Ma, Z.; Ke, Y.; Hu, Y. *Polym. Int.* **2003**, *52*, 1546. (k) Bluhm, M. E.; Folli, C.; Döring, M. *J. Mol. Catal. A* **2004**, *212*, 13. (l) Schmidt, R.; Hammon, U.; Gottfried, S.; Welch, M. B.; Alt, H. G. *J. Appl. Polym. Sci.* **2003**, *88*, 476. (m) Britovsek, G. J. P.; Cohen, S. A.; Gibson, V. C.; Maddox, P. J.; van Meurs, M. *J. Am. Chem. Soc.* **2004**, *126*, 10701. (n) Chen, Y.; Qian, C.; Sun, J. *Organometallics* **2003**, *22*, 1231. (o) Zhang, Z.; Zou, J.; Cui, N.; Ke, Y.; Hu, Y. *J. Mol. Catal. A* **2004**, *219*, 249. (p) Zhang, Z.; Chen, S.; Zhang, X.; Li, H.; Ke, Y.; Lu, Y.; Hu, Y. *J. Mol. Catal. A* **2005**, *230*, 1. (q) Bianchini, C.; Giambastiani, G.; Guerrero Rios, I.; Mantovani, G.; Meli, A.; Segarra, A. M. *Coord. Chem. Rev.* **2006**, *250*, 1391. (r) Gibson, V. C.; Redshaw, C.; Solan, G. A. *Chem. Rev.* **2007**, *107*, 1745.

(7) Britovsek, G. J. P.; Clentsmith, G. K. B.; Gibson, V. C.; Goodgame, D. M. L.; McTavish, S. J.; Pankhurst, Q. A. *Catal. Commun.* **2002**, *3*, 207.

(8) Bryliakov, K. P.; Semikolenova, N. V.; Zudin, V. N.; Zakharov, V. A.; Talsi, E. P. *Catal. Commun.* **2004**, *5*, 45.

(9) Bouwkamp, M. W.; Lobkovsky, E.; Chirik, P. J. *J. Am. Chem. Soc.* **2005**, *127*, 9660.

(10) Scott, J.; Gambarotta, S.; Korobkov, I.; Budzelaar, P. H. M. *Organometallics* **2005**, *24*, 6298.

(11) Bart, S. C.; Chlopek, K.; Bill, E.; Bouwkamp, M. W.; Lobkovsky, E.; Neese, F.; Wieghardt, K.; Chirik, P. J. *J. Am. Chem. Soc.* **2006**, *128*, 13901.

(12) Deng, L.; Margl, P.; Ziegler, T. *J. Am. Chem. Soc.* **1999**, *121*, 6479.

(13) Khoroshun, D. V.; Musaev, D. G.; Vreven, T.; Morokuma, K. *Organometallics* **2001**, *20*, 2007.

(14) Scott, J.; Gambarotta, S.; Korobkov, I.; Budzelaar, P. H. M. *J. Am. Chem. Soc.* **2005**, *127*, 13019.

(15) (a) Mason, M. R.; Smith, J. M.; Bott, S. G.; Barron, A. R. *J. Am. Chem. Soc.* **1993**, *115*, 4971. (b) Sinn, H. *Macromol. Symp.* **1995**, *97*, 27. (c) Sinn, H.; Kaminsky, W., Hoker, H. Eds. *Alumoxanes: Macromolecular Symposia 97*; Hutig and Wepf: Heidelberg, Germany, 1995. (d) Reddy, S. S.; Sivaram, S. *Prog. Polym. Sci.* **1995**, *20*, 309. (e) Hackmann, M.; Rieger, B. *CATTECH* **1997**, *1*, 79, and references therein. (f) Chen, E. Y.; Marks, T. J. *Chem. Rev.* **2000**, *100*, 1391. (g) Bryant, P. L.; Harwell, C. R.; Mrse, A. A.; Emery, E. F.; Gan, Z.; Caldwell, T.; Reyes, A. P.; Kuhns, P.; Hoyt, D. W.; Simeral, L. S.; Hall, R. W.; Butler, L. G. *J. Am. Chem. Soc.* **2001**, *123*, 12009.

(16) (a) Becke, A. D. *J. Chem. Phys.* **1993**, *98*, 5648. (b) Lee, C.; Yang, W.; Parr, R. G. *Phys. Rev. B* **1988**, *37*, 785.

(17) Wadt, W. R.; Hay, P. J. *J. Chem. Phys.* **1985**, *82*, 284.

(18) Jaguar, version 7.0; Schrödinger, LLC, New York, 2007.

(19) (a) Friesner, R. *Chem. Phys. Lett.* **1985**, *116*, 39. (b) Friesner, R. *J. Chem. Phys.* **1986**, *85*, 1462. (c) Friesner, R. *J. Chem. Phys.* **1987**, *86*, 3522. (d) Ringnalda, M. N.; Won, Y.; Friesner, R. *J. Chem. Phys.* **1990**, *92*, 1163. (e) Ringnalda, M. N.; Belhadj, M.; Friesner, R. A. *J. Chem. Phys.* **1990**, *93*, 3397. (f) Langlois, J. M.; Muller, R. P.; Coley, T. R.; Goddard, W. A., III; Ringnalda, M. N.; et al. *J. Chem. Phys.* **1990**, *92*, 7488. (g) Friesner, R. *J. Phys. Chem.* **1988**, *92*, 3091.

(20) Glendening, E. D.; Badenhoop, J. K.; Reed, A. E.; Carpenter, J. E.; Bohmann, J. A.; Morales, C. M.; Weinhold, F. NBO 5.0; Theoretical Chemistry Institute, University of Wisconsin, Madison, WI, 2001.

(21) (a) Jansen, H. B.; Ros, P. *Chem. Phys. Lett.* **1969**, *3*, 140. (b) Boys, S. F.; Bernardi, F. *Mol. Phys.* **1970**, *19*, 553.

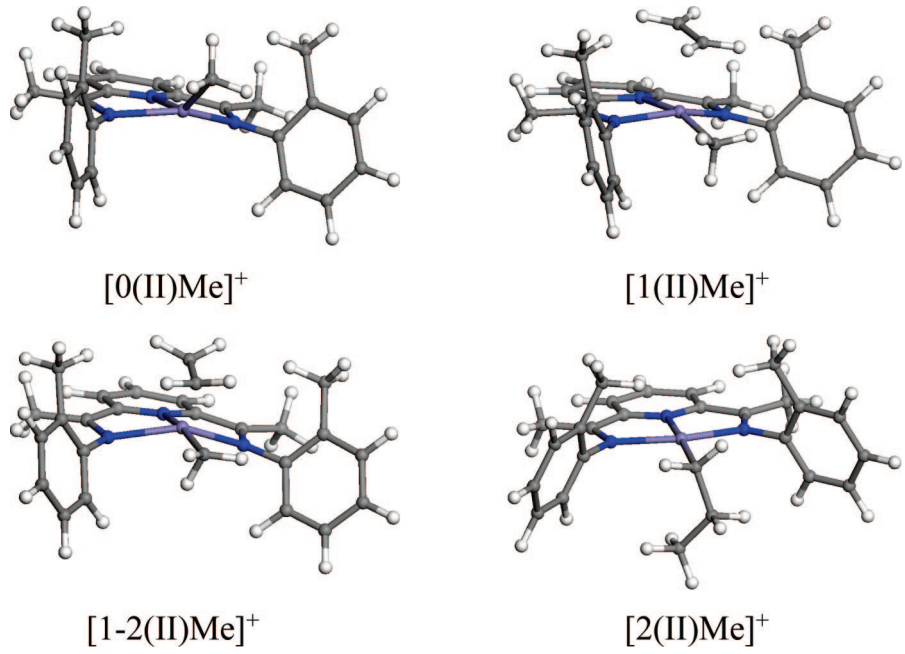

Figure 1. Optimized structures on the reaction path (initial structure: $[0(II)Me]^+$).

In this paper we adopt the following nomenclature: the first Arabic number (0, 1, 2) designates respectively the bare catalysts, the π-complexes, and the product in which the ethylene molecule is inserted into the Fe−Me bond. The label 1-2 designates the transition state for the insertion. The Roman number II or III refers to the oxidation state of the iron ion. Next, the substituents on the iron atom are marked: Me and/or Cl eventually extended with the subscript ax to indicate whether it occupies the axial position in the coordination sphere of Fe with respect to the N−N(pyridine)−N plane (no indication means that the substituent is in an equatorial position). The approach of the ethylene molecule is indicated by the terms anti (opposite side of methyl groups on phenyl substituents) or syn (the same side of methyl groups on phenyl subsituents), along with the signs $\perp$ and ||, which indicate the orientation of the ethylene molecule (perpendicular or parallel) with respect to the direction of the N(pyridine)−Fe bond. Finally, the atom numbering is given in Scheme 1.

3. Results and Discussion

With the iron bis(imino)pyridine dichloride precatalyst as the starting material (Scheme 1: R1 = R3 = R4 = H; R2 = Me; X1 = X2 = Cl), which reacts with the cocatalyst MAO, several structures have been proposed for the activated catalyst: the iron(III) species $[0(III)R]^{2+}$ and $[0(III)RCl]^+$ by Britovsek et al.,[7] the iron(II) systems $[0(II)Me]^+$ and $[0(II)Cl]^+$ by Castro et al.,[24] and $[0(II)Me]^-$ by Scott et al.[10,14] In this theoretical study we have investigated all of these potential activated species, together with six additional ones that can be formed from the same precursor. In all, 10 species were distinguished: four activated catalysts with oxidation state II, $[0(II)Me]^+$, $[0(II)Cl]^+$, $[0(II)Me]^-$, and $[0(II)Cl]^-$, and six with oxidation state III, $[0(III)Me]^{2+}$, $[0(III)Cl]^{2+}$, $[0(III)MeMe]^+$, $[0(III)ClCl]^+$, $[0(III)Me(syn)Cl]^+$, and $[0(III)ClMe(anti)]^+$. Each catalyst has been optimized with the ligand Me and/or Cl in either the equatorial or axial position.

Although, to the best of our knowledge, no olefin insertion has been observed into a metal−halogen bond, thus suggesting that a priori the species with only one chlorine atom (Fe(II) case) or two chlorine atoms (Fe(III) case) are probably not good candidates for ethene oligomerization, we have also considered these species to systematically study all possible activated catalysts. As an example, Figure 1 depicts the optimized structures for each step (0, 1, 1-2, 2) on the reaction path obtained starting from the $[0(II)Me]^+$ species.

A. Structure and Stability of Possible Activated Catalysts. a. The [0(II)] Species. i. The $[0(II)R]^+$ Species. Inspection of the geometrical data of the cationic $[0(II)R]^+$ species (Table S1; Supporting Information) shows a general increase of the bond lengths involving the Fe atom, upon increase of its spin multiplicity. The trend that these distances are more elongated in the quintet state than in the singlet might be explained by the partial occupation of all d orbitals in the first state, which in turn could imply a smaller donation of the n electrons of the nitrogen atoms into these d orbitals.

ii. The $[0(II)R]^-$ Species. For the anionic $[0(II)Me]^-$ and $[0(II)Cl]^-$ species, important differences are observed with respect to their cationic equivalents. The triplet states are the most stable configurations for the anions, whereas the quintet configurations are more stable for the cations. Furthermore, the energy differences between the different spin states significantly decrease in $[0(II)Cl]^-$. In contrast with the $[0(II)Cl]^+$ species, where the chloride ligand with its low-field properties attenuated the energy differences, thereby favoring high spins, this trend is not observed for the corresponding anion species. Since the Fe−Cl distance is significantly longer in the anion than in the cation, the ligand field due to the presence of the chloride ligand is even more reduced, and thus the low-spin configuration becomes relatively more stable.

iii. The $[0(III)R]^{2+}$ Species. The bond lengths in which the iron cation takes part do not vary significantly upon an increase of the multiplicity for the $[0(III)Me]^{2+}$ species (largest deviation

(22) Bader, R. F. W. *Atoms in Molecules*; Oxford University Press: New York, 1994.
(23) (a) Popelier, P. L. A. *Comput. Phys. Commun.* **1996**, *93*, 212. (b) Popelier, P. L. A. *Theor. Chim. Acta* **1994**, *87*, 465. (c) Popelier, P. L. A. *Mol. Phys.* **1996**, *87*, 1169. (d) Popelier, P. L. A. *Comput. Phys. Commun.* **1998**, *108*, 180. (e) Popelier, P. L. A. *Can. J. Chem.* **1996**, *74*, 829.
(24) Castro, P. M.; Lahtinen, P.; Axenov, K.; Viidanoja, J.; Kotiaho, T.; Leskelä, M.; Repo, T. *Organometallics* **2005**, *24*, 3664.

Table 1. Geometrical Data and Relative Electronic Energies for the Most Stable Bare Complexes

Fe(II) and Fe(III) species	M	Fe−N_{pyr} (Å)	Fe−N^1 (Å)	Fe−N^2 (Å)	Fe−X (Å)	rel energy (kcal/mol)
$[0(II)Me\text{-}ax]^+$	1	1.829	1.997	1.992	1.925	*+16.2*
$[0(II)Me]^+$	3	1.974	2.053	2.065	1.951	*+2.1*
$[0(II)Me]^+$	5	2.144	2.228	2.231	2.004	*0.0*
$[0(II)Cl]^+$	1	1.855	2.025	1.958	2.263	*+49.8*
$[0(II)Cl]^+$	3	1.917	2.038	2.041	2.192	*+10.6*
$[0(II)Cl]^+$	5	2.113	2.236	2.222	2.193	*0.0*
$[0(II)Me]^-$	1	1.820	1.932	1.931	2.010	*+26.6*
$[0(II)Me]^-$	3	2.057	2.203	2.201	2.063	*0.0*
$[0(II)Me]^-$	5	1.954	2.023	2.023	2.009	*+9.0*
$[0(II)Cl]^-$	1	1.883	1.976	1.976	2.298	*+2.6*
$[0(II)Cl]^-$	3	2.046	2.150	2.151	2.312	*0.0*
$[0(II)Cl]^-$	5	2.013	2.320	2.193	2.170	*+2.9*
$[0(III)Me\text{-}ax]^{2+}$	2	1.851	1.994	1.974	1.961	*+5.5*
$[0(III)Me]^{2+}$	4	2.008	2.070	2.075	1.962	*0.0*
$[0(III)Me]^{2+}$	6	2.080	2.090	2.091	2.056	*+12.3*
$[0(III)Cl]^{2+}$	2	1.903	2.231	2.007	2.027	*+7.5*
$[0(III)Cl]^{2+}$	4	2.108	2.238	2.245	2.187	*+0.2*
$[0(III)Cl]^{2+}$	6	2.098	2.221	2.230	2.196	*0.0*

Fe(III) species	M	Fe−N_{pyr} (Å)	Fe−N^1 (Å)	Fe−N^2 (Å)	Fe−X1/X2 (Å)	rel energy (kcal/mol)
$[0(III)MeMe]^+$	2	1.990	2.077	2.081	1.942/1.942	*+9.5*
$[0(III)MeMe]^+$	4	2.149	2.292	2.295	1.978/1.984	*0.0*
$[0(III)MeMe]^+$	6	2.142	2.256	2.256	2.047/2.051	*+10.3*
$[0(III)ClCl]^+$	2	1.926	2.032	2.033	2.169/2.232	*+22.6*
$[0(III)ClCl]^+$	4	1.970	2.067	2.065	2.231/2.248	*+12.4*
$[0(III)ClCl]^+$	6	2.120	2.206	2.204	2.200/2.209	*0.0*
$[0(III)MeCl]^+$	2	1.921	2.061	2.062	1.971/2.186	*+12.2*
$[0(III)MeCl]^+$	4	2.082	2.177	2.186	2.014/2.221	*0.0*
$[0(III)MeCl]^+$	6	2.139	2.235	2.235	2.070/2.234	*+4.7*
$[0(III)ClMe]^+$	2	1.911	2.056	2.028	2.190/1.981	*+9.0*
$[0(III)ClMe]^+$	4	2.092	2.204	2.205	2.223/2.025	*0.0*
$[0(III)ClMe]^+$	6	2.142	2.239	2.237	2.221/2.073	*+3.3*

0.24 Å; see Table 1). The quartet state is more stable than the sextet, while the lowest spin state (doublet) has the highest energy. In contrast with the case for its Fe(II) homologue, the presence of a chloride ligand in $[0(III)Cl]^{2+}$ diminishes the energy difference between the spin states and the quartet and sextet states are virtually degenerate. When the spin state is changed, important geometrical rearrangements with respect to the Fe(III) species with the methyl group substituent are observed: a decrease to about 60° for the dihedral angles ($C_{imino}{}^1-N^1-C^1{}_{aryl}{}^1-C^2{}_{aryl}{}^1$ and $C_{imino}{}^2-N^2-C^3{}_{aryl}-C^4{}_{aryl}$) with a sextet configuration and one axial conformer in the doublet state (Table S2; Supporting Information) and an increase of the bond lengths around the iron center for all the electronic states, except for the equatorial conformer of the doublet state. The energetically most stable structure remains the sextet state with the "most opened" structure around to iron, in which the two methyl groups on the aryl groups are bent away from each other.

iv. The $[0(III)R_2]^+$ Species. In comparison with the mono-substituted species, the dimethyl-substituted $[0(III)MeMe]^+$ iron cation complex undergoes an orbital reorganization, since the geometrical structure around the iron center has now become a "square-base pyramid" type (Figure 2). As the quartet spin state is the most stable state (Table 1), it can thus be said that further spin pairing to obtain a doublet configuration out of the quartet becomes less favorable. However, promoting an additional electron from the doubly occupied d_{yz} orbital (quartet) to occupy the d_{z^2} orbital (which is the least populated), resulting in a sextet configuration, yields the least stable state.

In the case of the Fe(III) complex with two chloride ligands, $[0(III)ClCl]^+$, the sextet state is the most stable configuration (Table 1), since the weaker chloride ligands destabilize to a lesser extent the d_{z^2} and $d_{x^2-y^2}$ orbitals, and thus the electrons prefer to stay unpaired. In comparison with the dimethyl homologue, the bond lengths are more contracted around the iron center.

These two mixed species $[0(III)MeCl]^+$ and $[0(III)ClMe]^+$ adopt a "square-base pyramid" structure, and the quartet state is the most stable configuration (Table 1). If the chloride ligand occupies the syn position, i.e. on the same side as the methyl groups on the phenyl substituents ($[0(III)ClMe]^+$), we note a flattening of the energy levels of the different spin states (Table S3; Supporting Information). It can also be noted that the repulsive interactions between the hydrogen atoms of the methyl groups on the phenyl substituents and those on the methyl group

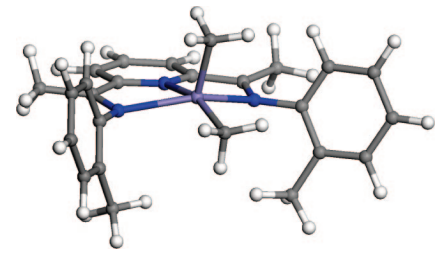

Figure 2. "Square-base pyramid" structure of Fe(III) bis(imino)pyridine with two methyl groups on iron.

Table 2. Geometrical Data and Coordination Energies of Fe(II) and Fe(III) π-Complexes

Fe(II) and Fe(III) species	M	Fe−N_{pyr} (Å)	Fe−N^1 (Å)	Fe−N^2 (Å)	Fe−C^1/C^2 (Å)	C^1=C^2 (Å)	coord energy (kcal/mol)
$[1(II)Me]^+$...anti∥	1	1.930	2.072	2.072	2.087/2.097	1.394	*−23.2*
$[1(II)Me]^+$...anti∥	3	1.982	2.090	2.086	2.626/2.484	1.348	*−4.0*
$[1(II)Me]^+$...anti∥	5	2.163	2.286	2.289	2.721/2.607	1.344	*−6.1*
$[1(II)Me]^+$...syn∥	5	2.163	2.316	2.304	2.551/2.571	1.347	−6.6
$[1(III)Me\text{-}ax]^{2+}$...anti∥	2	1.893	2.044	2.034	2.389/2.448	1.351	*−13.1*
$[1(III)Me]^{2+}$...anti∥	4	2.047	2.113	2.109	2.613/2.579	1.350	*−8.6*
$[1(III)Me]^{2+}$...anti∥	6	2.104	2.187	2.188	2.607/2.484	1.352	*−13.7*
$[1(II)Cl]^+$...anti∥	1	1.899	2.210	2.053	2.231/2.188	1.369	*−35.3*
$[1(II)Cl]^+$...anti∥	3	1.923	2.059	2.060	2.845/2.716	1.343	*−7.9*
$[1(II)Cl]^+$...anti⊥	5	2.158	2.287	2.289	2.518/2.518	1.348	*−10.7*
$[1(III)Cl]^{2+}$...anti∥	2	1.903	2.033	2.032	2.828/2.701	1.344	*−8.8*
$[1(III)Cl]^{2+}$...anti⊥	4	2.086	2.278	2.283	2.535/2.533	1.349	*−16.7*
$[1(III)Cl]^{2+}$...syn∥	6	2.102	2.170	2.172	2.465/2.653	1.353	*−14.4*
$[1(II)Me]^-$...anti∥	1	1.929	2.007	2.009	2.193/2.213	1.381	*−21.3*
$[1(II)Me]^-$...anti⊥	1	1.916	1.999	1.999	2.059/2.073	1.395	*−6.3*
$[1(II)Me]^-$...syn⊥	1	1.920	2.016	2.010	2.072/2.073	1.392	*−0.2*

on the iron cation are minimized in this configuration, while attractive H−Cl interactions of the hydrogen atoms of the methyl substituents on the aryl groups stabilize the energy of the structure with Cl in the syn position.

b. The π-Complexes. i. The $[1(II)Me]^+$ Species. The geometrical data and the relative energies for the coordination step of an ethylene molecule to the iron center are reported in Tables S4 and S5 (Supporting Information). Different approaches (anti and syn) of the ethylene molecule have been considered, but not all of them led to a minimum on the potential energy surface (PES). Generally, it is seen that the bond lengths involving the iron center are longer for each of the electronic states with respect to those in the bare catalyst structures (Table 1).

For the anti approach, it appears that the coordination of an ethylene molecule is energetically more favorable for the low-spin states (singlet) than for the high-spin states (triplet or quintet). The singlet configuration becomes relatively more stable, which could be interpreted as a form of spin quenching (Table 2). The elevated coordination energy calculated for the singlet state (−23.1 kcal/mol) is consistent with the observed elongation of the C−C bond of the ethylene molecule (from 1.331 to 1.394 Å) in the singlet state, resulting from the electron back-donation from the metal and the relatively short bond lengths between Fe and carbon atoms of the ethylene molecule (Fe−C^1/C^2 = 2.087 and 2.097 Å). The quintet state, however, remains the most stable configuration, followed by the triplet state. The ethylene molecule weakly coordinates to the iron center in the quintet and triplet states: the Fe−C^1/C^2 bond lengths are relatively long (between 2.484 and 2.721 Å) and the back-donation is weak (the C=C bond length varies between 1.344 and 1.349 Å; see Table S4).

Clearly the parallel approach of the ethylene molecule with the methyl group in equatorial position seems to be the privileged from the point view of the back-donation: 2.087 Å is the smallest value for the Fe−C^1 bond lengths and 1.394 Å is the largest value for the C=C bond lengths (Table S4).

It appears that there are several (local) minima on the PES in the case of a syn approach of the ethylene molecule. The singlet state exhibits again a strong coordination energy (−20.7 kcal/mol in Table S5) and also an important back-donation is seen: the Fe−C^1 bond length is about 2.082 Å, and the C=C bond length is about 1.395 Å. Yet the quintet state $[1(II)Me]^+$...syn∥ is the most stable state (Table 2). The observed spin quenching is consistent with the destabilization of the d_{z^2} orbital in the transition from a "square-planar" structure (complex type 0) to a "square-base pyramid" structure (complex type 1), which favors low spin states.

Energetically, it is difficult to clearly distinguish the preferred approach. Indeed, the two most stable quintet states (anti approach and syn approach) are close in energy (Table 2 and Scheme 2). *Thus, for the Fe(II)Me$^+$ species it seems that no preferential coordination mode exists for the ethylene molecule*.

ii. The $[1(III)Me]^{2+}$ Species. Tables S6 and S7 (Supporting Information) report the geometrical data and the relative energies for the coordination of ethylene for the $[1(III)Me]^{2+}$ species. Independent of how, syn or anti, the ethylene molecule approaches, the most favorable reaction energy is observed for the sextet configuration (−13.7 kcal/mol, Table 2), yet the quartet spin states remain the most stable ones.

The syn approach reveals the shortest bond lengths for the Fe−C^1/C^2 bonds for the doublet configuration $[1(III)Me]^{2+}$...syn∥ (2.138/2.174 Å), although interestingly, the quartet electronic configuration $[1(III)Me]^{2+}$...syn⊥ presents the strongest elongation of the C=C bond (1.427 Å), in spite of the longer Fe−C^1/C^2 bond lengths (2.609/2.573 Å).

In comparison with the case for the Fe(II) homologues, the coordination energies are slightly more exothermic (−8.6 kcal/mol versus −6.6 kcal/mol). This corroborates the recent theoretical work in which the Fe(III) was calculated to be the stronger electrophilic center on the basis of (DFT) Fukui functions.[25] However, this preliminary result is not sufficient to conclude the full reactivity of the metallic center.

iii. The $[1(II)Cl]^+$ and $[1(III)Cl]^{2+}$ Species. The geometrical data and the relative energies for the coordination step of ethylene for the $[1(II)Cl]^+$ species are reported in Tables S8, S9, S11, and S12 (Supporting Information). The reaction is more exothermic for the low spin states, but the high spin states remain the most stable species. Energy differences between the electronic states are smaller as a result of the weaker electric field of the chloride ligand as compared to the methyl group.

A particular structure has been localized for the singlet conformer $[1(II)Cl\text{-}ax]^+$...anti⊥. Indeed, we observe an important rotation of one phenyl substituent which allows the formation of a weak H-agostic bond between the iron ion and one

(25) Martinez, J.; Cruz, V.; Ramos, J.; Gutierrez-Oliva, S.; Martinez-Salazar, J.; Toro-Labbe, A. *J. Phys. Chem. C* **2008**, *112*, 5023.

Scheme 2. Enthalpy Variations for the Different Steps of the First Insertion Process for the [0(II)Me]$^+$ Species[a]

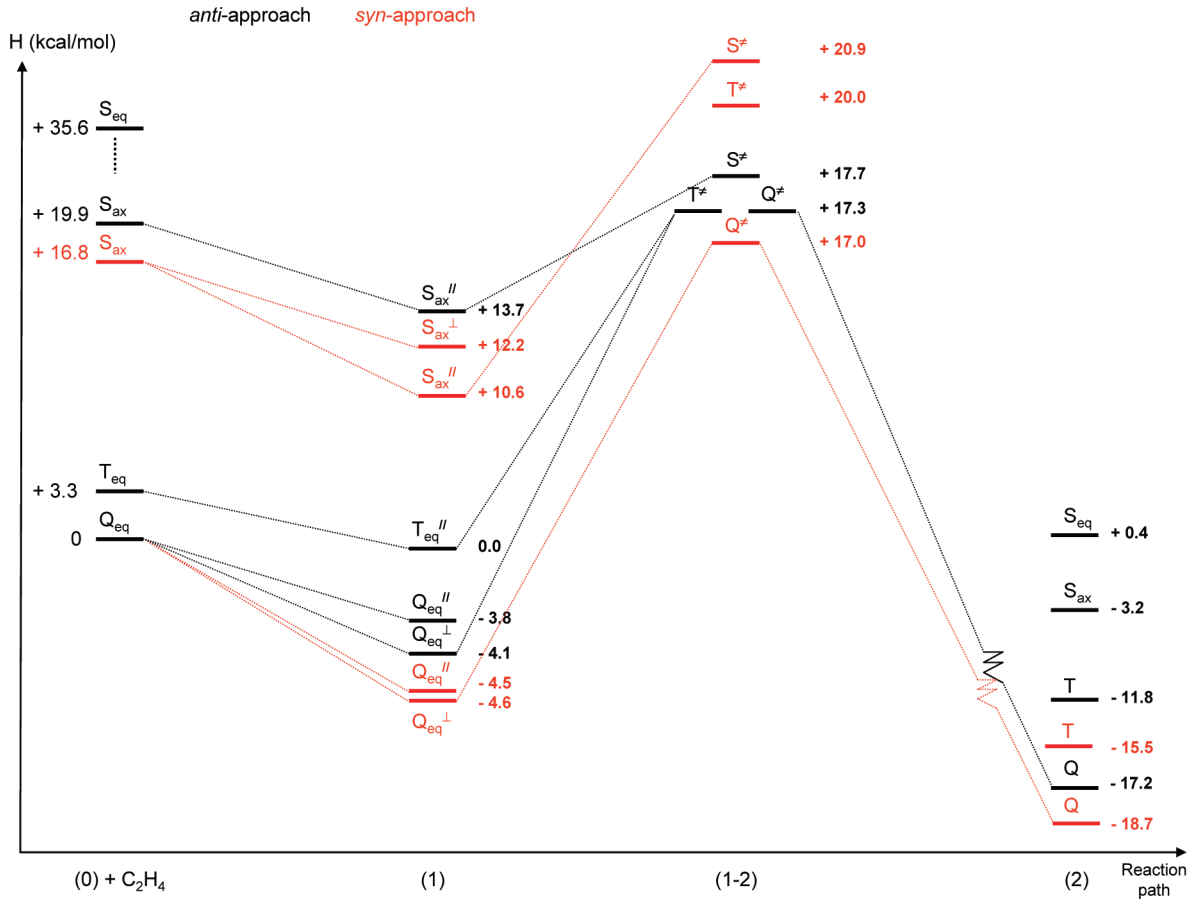

[a] Legend: S, singlet; T, triplet; Q, quintet.

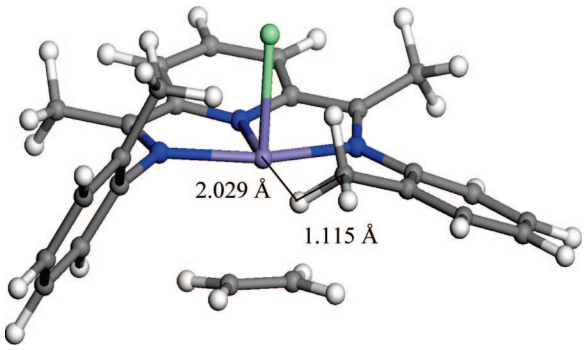

Figure 3. Octahedral structure of the singlet conformer [1(II)Cl-ax]$^+$...anti⊥

hydrogen atom of the methyl group (Figure 3).[26] Consequently, the iron cation has an octahedral environment which favors low spin states due to a destabilization of the d_{z^2} orbital and a stabilization of the d_{xy} orbital. Nevertheless, this octahedral conformation is not favorable for the ethylene molecule insertion, because the chloride ligand and the ethylene molecule are not on the same side of the plane defined by the bis(imino)pyridine ligand.

(26) On the basis of the results of the AIM calculations (see Table S25 with corresponding graph S25 in the Supporting Information) and the criteria for the definition of agostic bonds according to Popelier and Logothetis (Popelier, P. L. A.; Logothetis, G. *J. Organomet. Chem.* **1998**, *555*, 101.) it can be concluded that the interaction between the iron ion and hydrogen atom indeed corresponds to an agostic bond.

The quintet configuration is the most stable with a syn approach as compared to the anti approach and other spin states (Tables S8 and S9). For the [1(III)Cl]$^{2+}$ species the Fe−C^1/C^2 distances are important (between 2.344 and 2.893 Å) and also the back-donation is relatively weak: the C−C ethylene bond lengths vary from 1.340 Å to 1.358 Å (Tables S11 and S12).

iv. The [1(II)Me]$^-$ and [1(II)Cl]$^-$ Species. For the [1(II)Me]$^-$ and [1(II)Cl]$^-$species, the triplet state is the most stable state and the quintet state is the intermediate state, but not all theoretical coordinated forms could be localized for these electronic states. Inversely, the singlet state was calculated to have the highest energy and the only electronic state for which ethylene coordination was observed (Table S10, Supporting Information). After coordination the ethylene C−C bond lengths vary between 1.381 and 1.395 Å and the Fe−C^1/C^2 distances between 2.072 and 2.213 Å according to the coordination mode of the molecule. These atomic rearrangements, together with the contraction of the Fe−N bond lengths, indicate a firm coordination of the ethylene molecule. This assumption is furthermore supported by significant coordination energies for the two parallel approaches (−21.3 and −17.7 kcal/mol), although for the Fe(II)Me$^+$ and Fe(III)Me$^+$ singlet states even more exothermic coordination energies were calculated. In spite of numerous attempts, no ethylene coordination was observed for the [1(II)Cl]$^-$ species.

v. The [1(III)R$_2$]$^+$ Species. The coordination energies for the [1(III)MeMe]$^+$, [1(III)ClCl]$^+$, [1(III)MeCl]$^+$, and [1(III)ClMe]$^+$ species are shown in Tables S13 and S14 (Supporting Information). Whatever the ethylene molecule

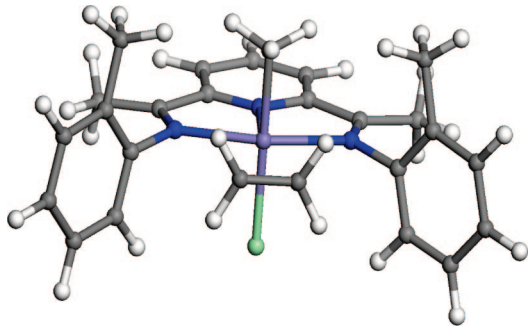

Figure 4. "Front-side" approach type for a disubstituted species.

approach (parallel, perpendicular, anti, syn), only an apparent coordination is observed for $[1(III)MeCl]^+$...anti|| with a quartet state with a coordination energy of −12.3 kcal/mol (Table S13). Nevertheless, a particular ethylene molecule approach exists for those species in which the ethylene molecule can coordinate to the iron ion between the two iron substituents: i.e., a "front-side" approach type (Figure 4). This approach shows the strongest coordination energies: −12.4 and −9.5 kcal/mol, respectively, for the quartet and doublet spin configurations of $[1(III)MeCl]^+$ (Table S13) and −8.3 and −7 kcal/mol for the doublet spin configurations of $[1(III)ClCl]^+$ and $[1(III)MeCl]^+$, respectively (Table S14).

On the basis of the results presented so far, either weak or no ethylene coordination was observed for the mono- and/or dichlorinated iron bis(imino)pyridine complexes. Since, to the best of our knowledge, no experimental data are available in which ethylene insertion into the Fe−Cl bond was described, these species will no longer be considered.

Since a comparison on its own of the calculated coordination energies does not allow us to arbitrate between the reactivities of the monomethylated Fe(II) or Fe(III) species, we will present in the following section the full reaction path for ethylene insertion and the feasible termination reactions.

B. Reaction Path for the $[0(II)Me]^+$ and $[0(III)Me]^{2+}$ Catalysts. a. Transition States for the Insertion Step. Since, either the transition could not be found, or the transition state was characterized by an imaginary frequency that did not correspond to the carbon-carbon bond formation, the anionic $[0(II)Me]^-$ species and the disubstituted Fe(III) species possessing one or two methyl substituents, were no longer considered.

Schemes 2 and 3 present the relative enthalpies of different process steps (0, 1, 1-2, 2) for the catalysts two monomethylated iron cations with respect to their bare catalysts: $[0(II)Me]^+$ and $[0(III)Me]^{2+}$.

The geometrical data, the relative energies, and the activation energies for the transition states of the $[1\text{-}2(II)Me]^+$ species for the anti and syn approaches are reported in Table 3, and additional details can be found in Tables S15 and S16 (Supporting Information).

In the case of an anti approach, the quintet, triplet, and singlet transition-state structures have practically the same enthalpy. In the case of the syn approach, the quintet remains the most

Scheme 3. Enthalpy Variations for the Different Steps of the First Insertion Process for the $[0(III)Me]^{2+}$ Species[a]

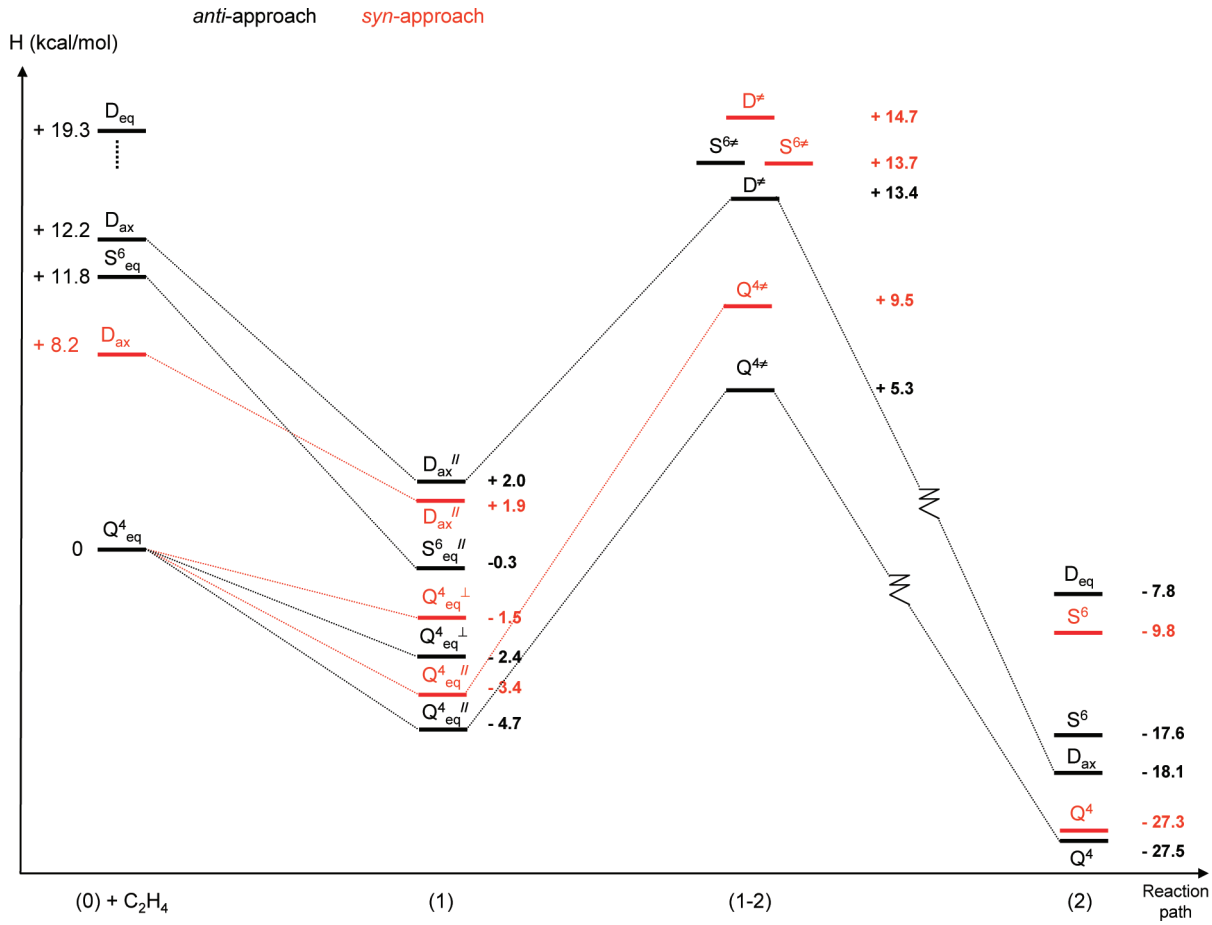

[a] Legend: D, doublet; Q^4, quartet, S^6, sextet.

Table 3. Geometrical Data, Relative Electronic Energies, and Activation Energies of Fe(II) and Fe(III) Transition States

Fe(II) and Fe(III) species	M	Fe−N_{pyr} (Å)	Fe−N^1/N^2 (Å)	Fe−C^1/C^2 (Å)	C^1=C^2 (Å)	C^2−Me (Å)	Fe−Hα (Å)	Δ*E* (kcal/mol)	rel energy (kcal/mol)
[1-2(II)Me]$^+$...anti|	1	1.870	2.042/2.042	1.978/2.134	1.440	2.059	1.942	3.9	0.0
[1-2(II)Me]$^+$...anti|	3	1.907	2.165/2.164	2.057/2.286	1.425	2.059	2.100	17.5	+0.8
[1-2(II)Me]$^+$...anti|	5	2.130	2.251/2.264	2.139/2.393	1.412	2.182	2.171	22.2	+1.3
[1-2(II)Me]$^+$...syn|	1	1.873	2.060/2.059	1.979/2.129	1.441	2.060	1.941	10.5	+2.8
[1-2(II)Me]$^+$...syn|	3	1.904	2.161/2.167	2.057/2.278	1.426	2.056	2.090	18.5	+2.5
[1-2(II)Me]$^+$...syn|	5	2.132	2.247/2.241	2.186/2.379	1.402	2.175	2.201	22.4	0.0
[1-2(III)Me]$^+$...anti|	2	1.941	2.025/2.056	2.121/2.281	1.398	2.352	2.036	13.6	+7.8
[1-2(III)Me]$^{2+}$...anti|	4	2.064	2.203/2.171	2.433/2.166	1.399	2.222	2.257	12.3	0.0
[1-2(III)Me]$^{2+}$...anti|	6	2.109	2.175/2.164	2.503/2.244	1.401	2.229	2.202	14.3	+9.2
[1-2(III)Me]$^{2+}$...syn|	2	1.936	2.074/2.057	2.126/2.291	1.389	2.390	2.117	7.9	0.0
[1-2(III)Me]$^{2+}$...syn|	4	2.089	2.198/2.200	2.160/2.409	1.403	2.204	2.370	12.9	+1.1
[1-2(III)Me]$^{2+}$...syn|	6	2.106	2.174/2.165	2.256/2.503	1.404	2.197	2.223	14.4	+7.4

favorable electronic state and the energy difference with the two other configurations is more important (3.0 kcal/mol). The activation enthalpies for both quintet states in the anti and syn approaches are very comparable, +21.4 and +21.6 kcal/mol, respectively. In the same way, the geometrical characteristics are quite similar (Fe−N_{pyr} bond lengths for the singlet state, 1.870 Å for the anti approach versus 1.873 Å for the syn approach; the N_{pyr}−Fe−X angle 162.87° for the anti approach versus 161.05° for the syn approach). The much smaller enthalpy barriers for the singlet states for the anti and syn approach of +4.0 and +10.3 kcal/mol, respectively, suggest an earlier transition state for these electronic configurations than for the higher spin states. This is indeed found upon analysis of the change in the C−C ethylene bond, which increases about 0.046 Å for syn and anti in the singlet state and 0.055 (syn) and 0.068 Å (anti) for the quintet state. Likewise, the Fe−$C_{ethylene}$ bond changes for the singlet are 0.103 Å (syn) and 0.109 Å (anti), whereas for the quintet state the changes are more important, 0.365 Å (syn) and 0.468 Å (anti).

As for the π-complexes, the Fe−N bond lengths are longer for the higher spin states. Interestingly, an agostic bond is formed between the iron and a hydrogen atom of the methyl substituent. This kind of interaction is found to be more important for the singlet states and decreases when the multiplicity increases. The (partial) empty d_{z^2} orbital in the low-spin configurations is thus available to accept electrons from the hydrogen atom and to form this H-agostic bond, deforming the "square-base pyramid" toward an octahedral type structure. This favorable interaction additionally explains the lower energetic barriers of the singlet transition of +4.0 (anti) and +10.3 kcal/mol for the syn approach reported in Table 3.

These results illustrate that (a) the two approaches, syn and anti, of the ethene molecule are equally likely to occur on the ground-state quintet PES, (b) excitation to the singlet or triplet spin state cannot be excluded, since the energy levels of the three spin states are nearly degenerate in the transition state, and (c) three principal geometrical structures are in dynamic evolution in this process: the square-planar structure, the square-based-pyramidal structure, and the octahedral structure.

The geometrical data, the relative energies, and the activation energies for the transition states of the syn and anti approaches for the [1-2(III)Me]$^{2+}$ species are reported in Table 3, and additional details are provided in Tables S17 and S18 (Supporting Information). In contrast to the case for their Fe(II) homologues, spin quenching seems to play a smaller role for the [1-2(III)Me]$^{2+}$ complexes, since in the anti approach, the quartet is clearly the most favorable transition state. Furthermore, for the Fe(III) species the anti approach is obviously preferred over the syn, since the "syn" transition state with a quartet state is 4.2 kcal/mol less stable. In comparison to the Fe(II) species, the reaction barrier is now considerably smaller, i.e., +10.0 kcal/mol, from which it can be concluded that the [Fe(III)Me]$^{2+}$ species is more active.

From a geometrical point of view, the bond lengths in the coordination sphere of iron are again longer when the multiplicity increases (except for the Fe−N_{imino} bond lengths). The shortest Fe−C^1/C^2 bond lengths are observed for the doublet states (2.121/2.281 Å (anti) and 2.126/2.291 Å (syn)), and the most opened dihedral angles are observed for the quartet states (−110.22/114.38 and −76.90/77.16°). Thus, on one hand the empty d orbitals in the doublet state allow a tighter binding of the ethylene molecule with the iron center, but on the other hand the more open structure in the quartet states facilitates the ethylene approach.

The observed Hα-agostic bond formation is most present in the doublet states, particularly for the anti approach (see Figure 5; Fe−Hα = 2.036 Å) and is weakest for the quartet states (2.257 Å for the anti approach and 2.370 Å for the syn approach). The low spin states thus induce the generated octahedral type structure.

b. Intermediates of the First Insertion Step. The geometrical data and the relative energies of the [2(II)propyl]$^+$ species in which the ethylene is now completely inserted are reported in Tables S19 and S20 (Supporting Information) and for the [2(III)propyl]$^+$ in Tables S21 and S22 (Supporting Information). Whatever the approach of the ethylene molecule (anti or syn), the quintet state is calculated to be the most stable state for the [2(II)propyl]$^+$ and the quartet state for the [2(III)propyl]$^{2+}$ catalyst. For both the [2(II)propyl]$^+$ and [2(III)propyl]$^{2+}$ species the difference in energy between the most stable spin configuration and the singlet and doublet states

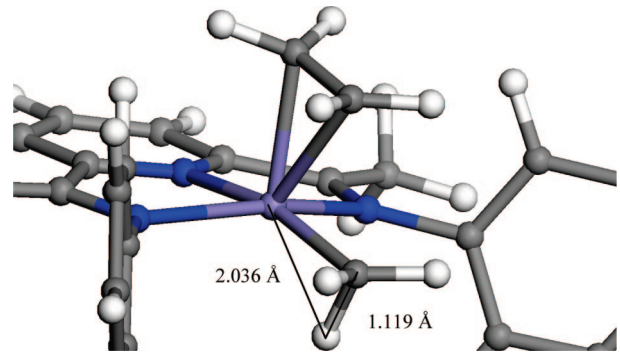

Figure 5. Hα-agostic bond for the doublet state in the anti approach (close view).

Table 4. Geometrical Data and Enthalpic and Electronic Energy Barriers of Transition States for the Termination Step (BHT versus BHE) of Fe(II) and Fe(III) Species

Fe(II) and Fe(III) species	M	Fe−H$^{\beta}$ (Å)	C$^{\beta}$−H$^{\beta}$ (Å)	C$^{=}$−H$^{\beta}$ (Å)	C=C (Å)	$\Delta H^{\ddagger}$ (kcal/mol)	$\Delta E_{SCF}{}^{\ddagger}$(kcal/mol)
				BHT			
[2(II)propyl]$^{+}$...anti‖	1	1.552	1.599	1.596	1.414	*+11.9*	*+13.0*
[2(II)propyl]$^{+}$...syn‖	3	1.547	1.651	1.641	1.408	*+17.4*	*+20.3*
[2(II)propyl]$^{+}$...syn‖	5	2.678	1.321	1.349	1.435	*+23.7*	*+25.4*
[2(III)propyl]$^{2+}$...syn‖	2	1.667	1.480	1.561	1.395	*+12.1*	*+13.4*
[2(III)propyl]$^{2+}$...syn‖	4	*a*					
[2(III)propyl]$^{2+}$...syn‖	6	*a*					
				BHE			
[2(II)propyl]$^{+}$...H$^{\beta}$	1	1.50	1.551			*+21.2*	*+23.3*
[2(II)propyl]$^{+}$...H$^{\beta}$	3	1.544	1.871			*+19.4*	*+21.3*
[2(II)propyl]$^{+}$...H$^{\beta}$	5	1.653	1.757			*+23.3*	*+25.3*
[2(III)propyl]$^{2+}$...H$^{\beta}$	2	1.473	1.677			*+17.9*	*+20.6*
[2(III)propyl]$^{2+}$...H$^{\beta}$	4	1.539	1.945			*+19.4*	*+22.6*
[2(III)propyl]$^{2+}$...H$^{\beta}$	6	1.737	1.767			*+31.3*	*+35.6*

[a] No structures were localized on the corresponding PES.

(D_{ax}), respectively, diminishes. Part of the origin of this increased stability of the low-spin states can be found in agostic interactions that are more prominently present in the complexes with the propyl radical and are partly lacking with the methyl substituent.

Upon analysis of the geometries of the [2(II)propyl]$^{+}$ species, slightly greater bond lengths in the direct coordination sphere of the iron ion are observed with respect to the [0(II)Me]$^{+}$ complexes, except for the equatorial singlet conformer (anti approach). It is worth mentioning that in general the (dihedral) angles do not undergo important changes, except for the singlet equatorial conformer (anti approach), where a closing of the N_{pyr}−Fe−R angle is seen (from 172.2° for the bare catalyst to 124.4° for the product) and a closing of the dihedral angles $C_{imino}{}^{1}$−N^{1}−$C^{1}{}_{aryl}$−$C^{2}{}_{aryl}$ (from −108.8 to −68.7°) and $C_{imino}{}^{2}$−N^{2}−$C^{3}{}_{aryl}$−$C^{4}{}_{aryl}$ (from 110.0 to 62.8°). Furthermore, for the axial singlet conformers (anti and syn) the same dihedral angles change respectively from −67.8 to −104.6° and from 68.5 to 131.8° for the anti product and for the syn product from −123.2 to 71.4 and from 111.2 to 73.8°.

c. Termination Steps. The activation enthalpies and reaction enthalpies that have been calculated for the bimolecular β-hydrogen termination (BHT) reaction and β-hydrogen elimination (BHE) reaction for the Fe(II)-Me and Fe(III)-Me activated species are reported in Table 4, together with some geometrical features (note that only the most stable conformers are reported for each case). The activation barriers for BHE have been calculated with respect to the products [2(II)propyl]$^{+}$ and [2(III)propyl]$^{2+}$, while for the BHT reaction the barrier has been calculated with respect to the π-complex formed between ethylene and [2(II)propyl]$^{+}$ or [2(III)propyl]$^{2+}$. Upon comparison of the enthalpy barriers of both reaction types, independent of the spin configuration, the BHT is 8.3 kcal/mol more favorable for the Fe(II)-Me species. These termination reactions preferentially take place at low spin surfaces, where the empty d orbitals facilitate the hydride transfer. The lowest enthalpy barrier is calculated for the BHT (+11.9 kcal/mol), which is significantly lower than the barrier for ethylene insertion. If the second and other ethylene insertion reactions possess similar energy barriers, only short oligomers can be achieved on the basis of these theoretical results, which are in agreement with the results of Morokuma et al.,[13] who investigated analogous bis(imino)pyridine complexes using a QM/MM approach with the B3LYP functional.

The enthalpy barrier for the iron(III) species are comparable to those of the iron(II) species. The former species will likely produce, given the nearly equivalent barriers for insertion and termination reactions, small oligomers.

d. Energy Profile for the Reaction Path. Schemes 2 and 3 summarize the principal results concerning the energetic profile (in terms of ΔH) for the [0(II)Me]$^{+}$ and [0(III)Me]$^{2+}$ species.[27] For both species, the enthalpy of ethylene coordination varies between −4 and −5 kcal/mol, independent of whether the ethylene arrives from the syn or the anti side. The energy barrier (+21.6 kcal/mol) computed for ethylene insertion for [0(II)Me]$^{+}$ is higher than that for the competing BHT termination reaction (+11.9 kcal/mol), thus suggesting that this species is likely not to be responsible for the experimentally observed oligomers.[28] In the case of [0(III)Me]$^{2+}$, a lower energy barrier for ethylene insertion is found (+10.0 kcal/mol), slightly lower than the concurrent BHT reaction (+12.1 kcal/mol). The complete insertion reaction is thermodynamically driven, given the exothermicity of −22.8 kcal/mol, along with the enthalpy change of +11.1 kcal/mol to decoordinate the formed olefin from the iron(III) center. On the basis of these overall results, oligomers are to be expected as the major product. These theoretical results calculated for the [Fe(III)Me]$^{2+}$ activated species are thus in agreement with the experimental results.

4. Conclusions

We have presented a theoretical DFT study, with the objective of better understanding the nature of the activated species that is responsible for the oligo-/polymerization of ethylene using an iron bis(imino)pyridine dichloride precursor. Accordingly, the oxidation states II and III in combination with all theoretical possible spin states of the iron ions have been considered, and the nature and number of substituents (Cl or Me) have been systematically varied as well.

It is found that *the disubstituted Fe(III) activated catalysts are not likely to be present as active species,* since for all the investigated species [0(III)MeMe]$^{+}$, [0(III)MeCl]$^{+}$, [0(III)MeCl]$^{+}$, and [0(III)ClCl]$^{+}$ low coordination energies have

(27) The corresponding Gibbs free energy variations (ΔG) have also been calculated: the BHT remains favorable with respect to the second monomer insertion in the case of Fe(II) species, while in the case of Fe(III) the second monomer insertion becomes even more favorable with respect to BHT.

(28) Babik, S. T.; Fink, G. *J. Organomet. Chem.* **2003**, *683*, 209.

been calculated. Only some significant favorable coordination interactions have been calculated. However, the corresponding transition states for insertion could not be located on the calculated PES.

The two most reactive activated species are the monomethyl-substituted $[0(II)Me]^+$ and $[0(III)Me]^{2+}$. Several modes of ethylene coordination have been studied, and on the basis of the coordination energy, the syn and anti approaches were found to be equivalent. These two catalysts show nearly equivalent enthalpies for ethylene coordination: −4.6 kcal/mol on the quintet PES and −4.7 kcal/mol on the quartet PES, respectively. The two dominant spin configurations remain the most stable spin states along the reaction pathway for ethylene insertion, although for the Fe(II)Me species the energy levels of the triplet and singlet state become nearly degenerate with the quintuplet state for the transition-state structure for ethylene insertion. The most favorable BHT termination reactions, on the other hand, occur on the singlet and doublet PES, respectively.

The ethylene insertion reaction is thermodynamically driven: $\Delta H = -14.1$ kcal/mol for $[Fe(II)Me]^+$ and $\Delta H = -22.8$ kcal/mol for $[Fe(III)Me]^{2+}$.

Since for the $[Fe(II)Me]^+$ species the activation enthalpy of the BHT termination reaction is much lower ($\Delta H^{\ddagger} = +11.9$ kcal/mol) than that for ethylene insertion ($\Delta H^{\ddagger} = +21.6$ kcal/mol), no oligomerization or polymerization activity of this species can be expected. However, for the $[Fe(III)Me]^{2+}$ activated species the ethylene insertion barrier of $\Delta H^{\ddagger} = +10.0$ kcal/mol, clearly suggesting higher activity with respect to its iron(II) homologue, is lower than its competing BHT termination reaction with a barrier of $\Delta H^{\ddagger} = +12.1$ kcal/mol. Since both barriers are of nearly equal magnitude, oligomers are to be expected, in good agreement with the experimental results.

Work is in progress to better understand why higher order olefins, such as propylene or butene, undergo specific insertion reactions (of the type (1,2) and/or (2,1)) to yield predominantly linear olefins.[28]

Acknowledgment. C.A. and R.R. thank the IFP for financial support. We also thank Drs. Ilaria Ciofini and Laurent Joubert (AIM calculations) from the ENSCP and Dr. Hélène Olivier-Bourbigou from the IFP for fruitful scientific discussions.

Supporting Information Available: Tables S1−S24, giving geometrical data and/or thermodynamic values of all the studied species, and Figure S25, giving a contour graph of $[1(II)Cl\text{-}ax]^+$...anti⊥. This material is available free of charge via the Internet at http://pubs.acs.org.

OM701122R